INSTITUTE OF PHYSICS PUBLISHING NANOTECHNOLOGY
Nanotechnology **17** (2006) 4163–4167 doi:10.1088/0957-4484/17/16/028

Formation of uniform and square nanopore arrays on (100) InP surfaces by a two-step etching method

A S Zeng[1], M J Zheng[1,3], L Ma[2] and W Z Shen[1]

[1] Laboratory of Condensed Matter Spectroscopy and Opto-Electronic Physics, Department of Physics, Shanghai Jiao Tong University, Shanghai 200240, People's Republic of China
[2] School of Chemistry and Chemical Technology, Shanghai Jiao Tong University, Shanghai 200240, People's Republic of China

E-mail: mjzheng@sjtu.edu.cn

Received 11 May 2006, in final form 10 July 2006
Published 1 August 2006
Online at stacks.iop.org/Nano/17/4163

Abstract
Uniform and square single-crystal InP nanopore arrays have been successfully fabricated on a (100) *n*-InP surface by a two-step etching method. The characteristic of slow etching rates in four equivalent crystalline (011) facets of (100) *n*-InP in a mixture of pure HCl and pure H_3PO_4 has been found, which is the main reason for the formation of square single-crystal InP nanopores. The distribution of nanopores can be closely associated with the distribution of carriers in the semiconductor during the electrochemical etching process. An oscillating behaviour of current has been observed, which can probably be attributed to the oscillations in concentration of the electrolyte at the pore tips caused by diffusion of the electrolyte in the nanopore channels.

After the discovery of visible photoluminescence in porous silicon [1], considerable interest has been focused on the investigation of pore formation in semiconductors, especially in III–V semiconductors due to their potential applications in quantum devices and photonic-bandgap crystals [2], etc. Various methods for the self-formation of nanopore arrays have been established, among which electrochemical etching has proved to be a powerful tool for the fabrication of two-dimensional nanostructures on the surface of III–V semiconductors, such as InP in HCl [3–7], GaP in H_2SO_4 [8, 9], and GaAs in HCl and HF electrolytes [10, 11].

Due to its direct band gap (1.35 eV), InP exhibits very efficient optical recombination of charge carriers, which widens the range of possible applications such as lasers, light-emitting diodes, and solar cells. In addition, properties different from those of bulk InP were also found in porous InP. The nonlinear optical response of porous InP membranes was examined, which suggested that the enhanced nonlinear optical response was related to strong enhancements of the local field within the porous network [12]. Thanks to these good features, porous InP has been used to fabricate nanoscaled Schottky diodes [13], waveguides [14], etc. However, it is still an open challenge to obtain high-quality InP nanopore arrays. According to previous reports, the anodization condition has a significant effect on pore growth and morphology in porous InP. Tiginyanu *et al* [15] have observed the highest degree of order at 7–8 V in 7.5% HCl solution. Langa *et al* have reported that the growth direction of pores in InP strongly depended on the anodic current density [5]. Current-line oriented pores and crystallographically oriented pores were formed at high (60 mA cm^{-2}) and low (<5 mA cm^{-2}) current density anodization, respectively. Although nanopore arrays with an irregular top layer after anodization have been realized by several groups [3, 5], it is still a great challenge to remove the irregular top layer to obtain high-quality uniform InP nanopore arrays.

Here we report a new approach for the fabrication of uniform and square InP nanopore arrays on a (100) *n*-InP surface using a two-step etching method. The formation mechanism of nanopores has been investigated by using a three-electrode electrochemical analysis system, transmission electron microscope (TEM) and scanning electron microscope (SEM). It has been observed that the formation of an irregular top layer corresponds to the unstable current process, which

[3] Author to whom any correspondence should be addressed.

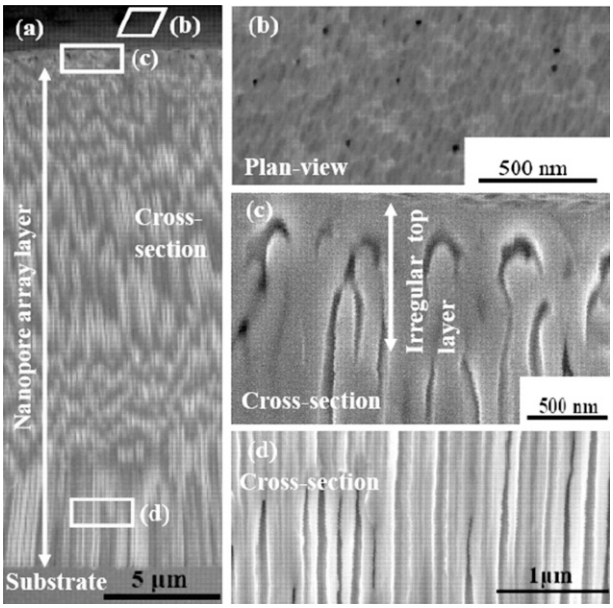

Figure 1. SEM images of nanopores prepared by electrochemical etching in 7.5% HCl electrolyte under $V = 7$ V and $t = 30$ s without removing the irregular top layer: (a) cross section of the overall pore structure; (b) surface of the irregular top layer; (c) cross section of the irregular top layer; and (d) cross section of the nanopore array layer.

could be explained by the initial non-uniform distribution of carriers in the surface of the semiconductor.

The porous InP layer was fabricated through an anodizing electrochemical procedure with Sn-doped InP ($>1 \times 10^{18}$ cm^{-3}) wafers (with an etch pit density of about 5×10^4 cm^{-2}) as the anode in a 7.5% HCl electrolyte. Prior to each experiment, the wafers were degreased with acetone and extensively rinsed with deionized water and then blown dry in N_2. The wafers were then pasted onto the centre of circinal sheet copper using silver paste, while the exposed part of the circinal sheet was covered with insulating paint. An O-ring was pressed against the wafer when the circinal sheet copper was screwed down into a Teflon electrochemical cell as the anode. Accordingly, graphite was used as the cathode. An anodic polishing was carried out using an electrolyte of 0.3 M oxalic acid under an anodizing voltage of 26 V at 20 °C for 3 min to smooth the surface of the wafer. Then the anodization lasted for 30 s in 7.5% HCl electrolyte under a constant anodizing voltage of 7 V and an electrolyte temperature of 20 °C. The specimen was then immersed in a mixture of pure HCl and pure H_3PO_4 (V_{HCl}:V_{H3PO4} = 1:3) at 20 °C for 6 min to remove the irregular top layer. After ultrasonic washing in deionized water for 3 min, uniform and square nanopore arrays were formed on the (100) InP surfaces.

An SEM system (Sirion 200) was used to analyse the morphology characterization of the porous samples. A TEM system (JEM-100CX) was used to analyse the microstructure of the nanopore arrays. An electrochemical analysis system (CHI618B) was utilized to study the anodic etching process in detail. Moreover, an x-ray diffraction (XRD) spectrum was obtained using a Bruker D8 ADVANCE system.

Figure 1 shows cross-sectional and plan-view SEM images of the porous sample formed in 7.5% HCl electrolyte.

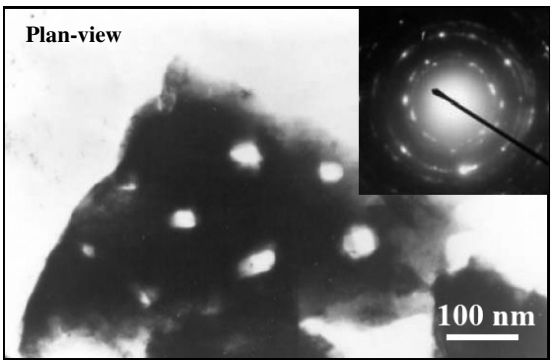

Figure 2. Plan-view TEM image and SAED pattern of the irregular top layer.

A multilayer structure, including the irregular top layer, the nanopore array layer, and the substrate, can be seen in figure 1(a). The pores in the irregular top layer are sparse, with a pore diameter of about 25 nm, as seen in figure 1(b). Also, the thickness of the irregular top layer is $\sim$1 μm, as estimated from figure 1(c). Below this layer, nanopores with straight pore walls were formed, as shown in figure 1(d). The pores at the interface between the irregular top layer and the nanopore array layer are connected. It should be noted that the cross section of the porous sample was prepared by mechanical cutting, and it was difficult to obtain a smooth cross section (see figure 1(a)). In fact, the nanopore channels in the nanopore array layer are all perpendicular to the sample surface and ending at the same interface.

By repeating this electrochemical etching process, we find that the multilayer structure can be reproduced. To analyse its microstructure further, the irregular top layer was mechanically scraped off and then skived in a mortar with a small quantity of anhydrous ethylalcohol to obtain thin foils necessary for TEM. Figure 2 shows the plan-view TEM image and the selected-area electron diffraction (SAED) pattern of the irregular top layer. The irregular top layer is polycrystalline InP, as indicated by figure 2. However, to realize the use of the nanopore array layer in optoelectronic devices, it is very necessary to remove the irregular top layer. Until now, two main methods have been used to remove the irregular top layer: the mechanical method [6] and the over-potential method during the anodization process [3]. Unfortunately, some difficulties still exist with these two methods. With mechanical remove, the top layer can be totally removed, but the nanopore array layer can be easily damaged. Using the over-potential method during the anodization process, the morphology of the nanopores is not very uniform and large fluctuations still exist in the pore size and pore wall thickness.

We found that, by using a wet etching method as well as ultrasonic washing in deionized water, uniform and square InP nanopore arrays can be obtained after removing the irregular top layer. Figures 3(a)–(c) display plan views of sample etching in a mixture of pure HCl and pure H_3PO_4 (V_{HCl}:V_{H3PO4} = 1:3) for 4 min, 6 min, and 8 min, respectively. The irregular top layer cannot be totally removed for the sample etched for 4 min, while both of the upper two layers are completely removed for the sample etched in the mixture for 8 min. When the etching time is 6 min, uniform and square

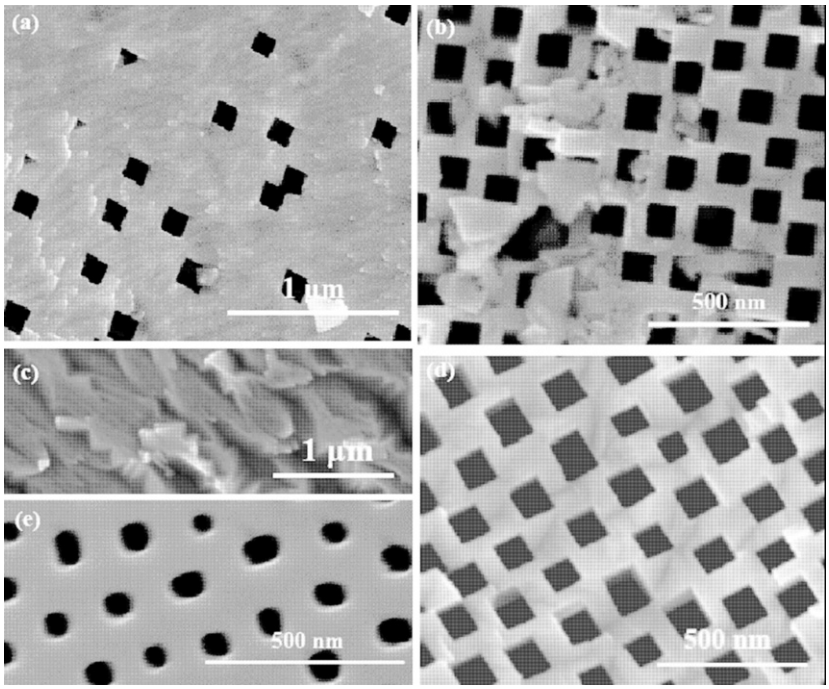

Figure 3. SEM images of nanopores formed over different wet etching times: (a) 4 min, (b) 6 min, (c) 8 min and (d) 6 min, without being ultrasonically washed except for (d). Also, (e) shows a plan view of the nanopore array layer formed after only the first step of the electrochemical etching process and by decoating the top layer by mechanical cutting.

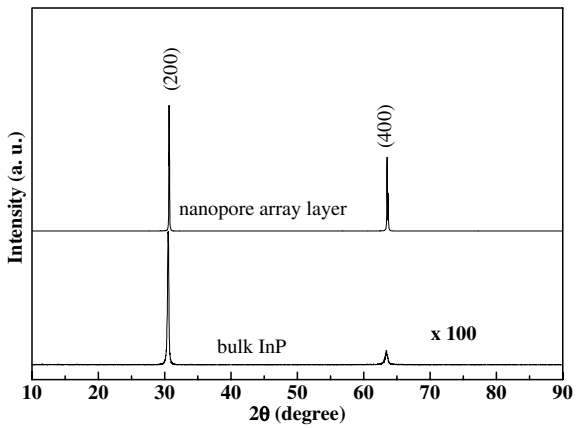

Figure 4. XRD spectra of bulk InP and nanopore array layer.

InP nanopore arrays were observed, and the thickness of the nanopore array layer was approximately 18 μm. However, some small particles were still adsorbed on its surface, as shown in figure 3(b). To obtain a clean surface, an ultrasonic wave was employed to remove the small particles on the surface of the nanopore arrays in deionized water for 3 min. Figure 3(d) shows an SEM image of the sample after wet etching in the mixture for 6 min at 20 °C as well as ultrasonic washing. It shows that the small particles absorbed on the porous layer were totally removed, which realized high cleanliness on the sample surface. Uniform and square nanopores defined by four equivalent crystalline (011) facets (which will be proved later) were formed over a large area on the surface. The average pore area, the average pore wall thickness and the pore density are 108 × 108 nm^2, 80 nm and 3.1 × 10^9 cm^{-2}, respectively. In contrast, the plan view (figure 3(e)) of the nanopore array layer after removing the irregular top layer using the mechanical cutting method shows that the shape of the nanopores is irregular, and the average pore diameter and the average pore wall thickness were estimated to be 75 nm and 120 nm, respectively. This clearly indicates that the second wet etching process plays a key role in the formation of uniform and square nanopore arrays.

An XRD measurement was carried out to evaluate further the quality of the uniform and square nanopore array layer. Figure 4 shows the XRD spectra of the bulk InP and the square nanopore array layer, both of which exhibit two diffraction peaks at $2\theta = 30.52°$ and 63.41°, indicating that no new phase was generated during the wet etching process. Figure 5 shows the TEM image and the SAED pattern of the nanopore array layer, revealing that the square nanopore array layer is single-crystalline InP. Moreover, each of the square nanopores is defined by four equivalent crystalline (011) facets, which indicates that InP is slowly etched on the four crystalline facets in a mixture of pure HCl and pure H_3PO_4.

The above results indicate that square single-crystal InP nanopore arrays can be realized in a self-organized fashion by a two-step etching method. The formation of the square nanopores results from both of the two-step etching processes, while the space distribution of the nanopore arrays is only determined by the first electrochemical etching process. As a result, it is also necessary to analyse further the formation mechanism of the nanopore arrays during the electrochemical etching process.

Current–time (I–t) curves were recorded with a three-electrode electrochemical analysis system (CHI618B) under

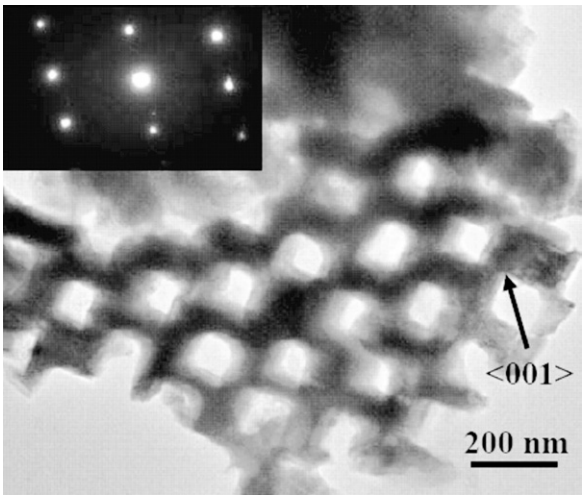

Figure 5. The TEM image and SAED pattern of the nanopore array layer.

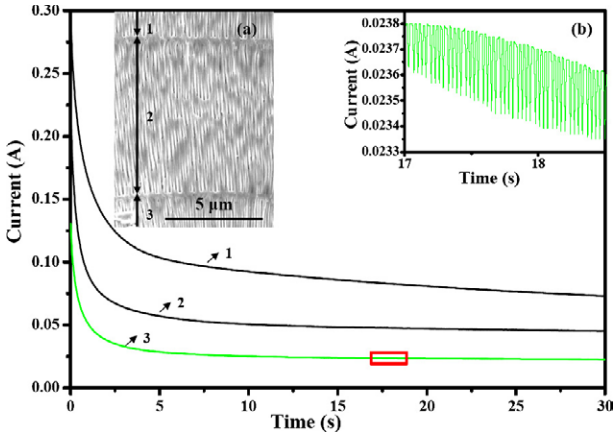

Figure 6. Current–time curves obtained during anodization by switching the anodization current on and off three times, with each current-off time being 0.5 min. (a) The inset SEM image shows part of the corresponding cross-sectional view of the sample (symbols 1, 2 and 3 correspond to the first 30 s, the second 30 s and the third 30 s, respectively.). (b) The inset *I–t* curve shows the oscillation of currents enlarged from the square marked in the *I–t* curve 3.

(This figure is in colour only in the electronic version)

a constant potential of 7 V to investigate the process of electrochemical anodization, as shown in figure 6. During the first 30 s (curve 1), the current was larger than 0.28 A at first, then decreased sharply with increasing etching time until the etching time was 5 s, while the current was less than 0.10 A. After that, the current became more stable with increasing etching time. It should be recognized that the formation of porous InP is a dissolution process and not a growth phenomenon, and that the number of carriers in the sample is an important factor affecting the current. Therefore, the formation of random nanopores in the irregular top layer during the initial electrochemical etching process could be related to the impurity distribution in the III–V semiconductor. Moreover, due to the presence of defects (i.e. etch pits), the carrier density distribution may be different at the position of the defects, which could also be a reason for the formation of random nanopores in the irregular top layer [16]. When the electric field is applied to the sample surface, the place with a higher carrier density has a higher tendency to be dissolved and form nanopores. Due to the non-uniform distribution of carriers on the surface of the semiconductor, nanopores with an irregular distribution are also produced on the sample surface at the beginning of etching. Once a pore has been initiated, the electric field is enhanced by the curvature of the surface [16]. Therefore, after the initial pitting of the surface, further etching proceeds not only in the pore tips, but also on the sidewalls of the nanopores because of remnant carriers on the nanopore walls, which increases the density of nanopores, as shown in figure 1(c). The amount of carriers participated in electrochemical etching decreases sharply along with the formation of the irregular top layer, which causes the dramatic decrease in current. From figure 6 (curve 1) we can conclude that the initial 5 s corresponds to the formation of the irregular top layer. After the initial 5 s, the carriers in the pore walls are nearly depleted, which causes the high resistance of the pore walls compared to bulk InP or the electrolyte [17]. Also, the carriers are redistributed in the nanopore tips due to the effect of the electric field. Thus the etching current preferentially flows down the electrolyte in the nanopores, leading to the occurrence of dissolution only at the pore tips. During this period, the nanopores are more uniform and the etching current is more stable. This formation process of multilayer structures in etched InP is similar to that in etched GaP proposed by Tomioka *et al* [18]. Accordingly, the anodic etching process could be divided into two periods: one for the formation of the irregular top layer (0–5 s) and the other for the formation of the nanopore array layer (5–30 s).

To confirm the above argument further, we applied the same etching process three times to the same sample. The electrical source was cut off for 0.5 min after the sample was etched for the first 30 s (phase 1), then turned on again for the second 30 s (phase 2) to measure the *I–t* curve under the same anodic potential of 7 V, as shown in figure 6 (curve 2). The *I–t* curve 3 (phase 3) of figure 6 was also obtained using the same method. It can be found that the three *I–t* curves reveal the same change in regulation. According to the above argument, the morphology of the etching layer formed in etch phases 2 and 3 should be the same as that formed in etch phase 1. This was further confirmed by the cross-sectional SEM image, as shown in figure 6(a). Note that this figure only showed part of the cross-sectional image, in which the irregular top layer formed in etch phase 1 and part of the nanopore array layer formed in etch phase 3 are not shown. It was found that the pores of phase 1 were not just made longer in phase 2. Instead, a new irregular layer was formed, followed by a new nanopore array layer. It looks as if the second and third 30 s etching processes started somewhere in the 'bulk'. This should be associated with the redistribution of carriers during the current-off time of 0.5 min, since there were no other changes in the process. It should be noted that the pores in the irregular layer (phase 2) were connected with some of the nanopore ends in phase 1, which can be observed from the larger multiple cross-sectional SEM image. Moreover, the etching thickness gradually decreased from etch phase 1 to etch phase 3, and the thickness of the irregular layer in etch phases 2 and 3 was also

thinner than that in etch phase 1. The above results indicate that the irregular layer is always formed at the beginning of the etching process, which also demonstrates the importance of finding a better way to remove the irregular top layer for the use of the nanopore arrays. Furthermore, these results imply that the space position, density, and uniformity of the nanopore arrays on the surface of the III–V semiconductor by the anodic etching method could be controlled by modulating the distribution of carriers in the semiconductor.

It is noted that an oscillation behaviour can be seen when the current–time curve is enlarged, as shown in figure 6(b). The average periodicity of current oscillations can be estimated to be 32.2 ms. Many kinds of oscillatory behaviours have been observed during electrochemical anodization of *n*-InP in different electrolytes, such as potential oscillations under constant current in HCl electrolyte [19] and current oscillations under constant potential in $(NH_4)_2S$ electrolyte [20]. It has been reported that the voltage oscillations are associated with intrinsic current oscillation together with some phase coupling or correlation between nanopores [19], and that the current oscillations correspond to the continuous growth of a thick porous film on the electrode [20]. However, most of the reports only described macroscopic phenomena of the anodization, which cannot explain the mechanism of instantaneous electrochemical anodization by a magnitude of milliseconds.

Here, the instantaneous current oscillations can probably be attributed to the oscillations in concentration of the electrolyte at the pore tips caused by the diffusion of the electrolyte in the nanopore channel. As anodization progresses, the reactant ions in the electrolyte close to the pore tips are depleted in a short time and the concentration of the electrolyte at this site decreases dramatically, which requires further reactant ions from the subsequent electrolyte in the nanopore channel to diffuse to the pore tips due to the effects of osmotic pressure and electric field to maintain the anodization. As a result, during anodization, the reactant species near the pore tips are depleted and supplied frequently, which generates the oscillations in concentration of the electrolyte as well as the current oscillations.

We have successfully fabricated uniform and square InP nanopore arrays on (100) *n*-InP surfaces by a two-step etching method. The space position, density, and uniformity of the nanopore arrays on the surface of the III–V semiconductor using the anodic etching method could be tuned by modulating the distribution of carriers in the semiconductor. The irregular top layer that appears during electrochemical anodization can be totally removed during a second step of the wet etching process using a mixture of pure HCl and pure H_3PO_4 together with ultrasonic washing. Both an appropriate etching time and the ultrasonic washing process are necessary and important to the formation of uniform and square InP nanopore arrays. Current oscillations have been observed, which can probably be attributed to the oscillations in concentration of the electrolyte at the pore tips caused by diffusion of the electrolyte in the nanopore channels.

Acknowledgments

This work was supported by the Natural Science Foundation of China grant no. 50572064 and the National Minister of Education Program for Changjiang Scholars and Innovative Research Team in University (PCSIRT).

References

[1] Canham L T 1990 *Appl. Phys. Lett.* **57** 1046
[2] Yablonovitch E 2000 *Science* **289** 557
[3] Fujikura H, Liu A, Hamamatsu A, Sato T and Hasegawa H 2000 *Japan. J. Appl. Phys.* **39** 4616
[4] Liu A and Duan C 2001 *Appl. Phys. Lett.* **78** 43
[5] Langa S, Tiginyanu I M, Carstensen J, Christophersen M and Föll H 2000 *Electrochem. Solid-State Lett.* **3** 514
[6] Langa S, Christophersen M, Carstensen J, Tiginyanu I M and Föll H 2003 *Phys. Status Solidi* a **197** 77
[7] Su G, Guo Q and Palmer R E 2003 *J. Appl. Phys.* **94** 7598
[8] Van Driel A F, Vanmaekelbergh D and Kelly J J 2004 *Appl. Phys. Lett.* **84** 3852
[9] Tjerkstra R W, Gomez Rivas J, Vanmaekelbergh D and Kelly J J 2002 *Electrochem. Solid-State Lett.* **5** G32
[10] Schmuki P, Lockwood D J, Labbe H J and Fraser J W 1996 *Appl. Phys. Lett.* **69** 1620
[11] Beji L, Sfaxi L, Benouada H and Maaref H 2005 *Phys. Status Solidi* a **202** 65
[12] Reid M, Cravetchi I, Fedosejevs R, Tiginyanu I M, Sirbu L and Boyd Robert W 2005 *Phys. Rev.* B **71** 081306
[13] Hasegawa H, Sato T and Kaneshiro C 1999 *J. Vac. Sci. Technol.* B **17** 1856
[14] Langa S, Lölkes S, Carstensen J, Hermann M, Böttger G, Tiginyanu I M and Föll H 2005 *Phys. Status Solidi* c **2** 3253
[15] Tiginyanu I M, Langa S, Christophersen M, Carstensen J, Sergentu V, Foca E, Rios O and Föll H 2002 *Mat. Res. Soc. Symp. Proc.* **692** K2.7.1
[16] Erné B H, Vanmaekelbergh D and Kelly J J 1996 *J. Electrochem. Soc.* **143** 305
[17] Beale M I J, Chew N G, Uren M J, Cullis A G and Benjamin J D 1985 *Appl. Phys. Lett.* **46** 86
[18] Tomioka K and Adachi S 2005 *J. Appl. Phys.* **98** 073511
[19] Langa S, Carstensen J, Tiginyanu I M, Christophersen M and Föll H 2001 *Electrochem. Solid-State Lett.* **4** G50
[20] Harvey E, Buckley D N and Chu S N G 2002 *Electrochem. Solid-State Lett.* **5** G22